

Screening and electrochemical detection of an antibiotic producing gene in bacteria on an integrated microchip

Cite this: *Anal. Methods*, 2013, **5**, 6814

Dawoon Han,^a Rohit Chand,^a Ik-Soo Shin^{*b} and Yong-Sang Kim^{*a}

We demonstrate the electrochemical determination of a secondary metabolite producing gene on an integrated microfluidic chip. The fabricated microchip was assembled with a continuous channel for polymerase chain reaction (PCR) and an electrochemical detector in order to achieve rapid and sensitive determination of the *valC* gene. *valC* is a gene responsible for producing antibiotic validamycin A in *Streptomyces hygroscopicus*. Biotin-conjugated primers amplified the *valC* gene. After the PCR, a DNA amplicon was analyzed in the electrochemical cell containing a streptavidin functionalized Au working electrode. The guanosine present in the DNA amplicon released electrons upon electrochemical oxidation at 0.93 V and the peak current linearly increased with the concentration of the captured DNA amplicon. The fabricated chip successfully amplified and detected the *valC* gene as low as 30 pg μL^{-1} resulting in a sensitive, portable and integrated DNA analysis for a secondary metabolite.

Received 2nd August 2013

Accepted 26th September 2013

DOI: 10.1039/c3ay41321g

www.rsc.org/methods

1. Introduction

Validamycin A is an antifungal antibiotic produced by *Streptomyces hygroscopicus* and used in East Asia as a crop protectant for the treatment of sheath blight disease of rice plants and damping-off of vegetables.¹ Validamycin A is a representative antibiotic of the C₇-N aminocyclitol family of natural products.² It is a non-systemic antibiotic that controls the spread of the pathogen by reducing the hyphal growth rather than degrading the fungi.³ Interest in such biological control of plant pathogens has increased considerably to minimize the use of hazardous chemical pesticides and also because it provides control of diseases that cannot or can only partially be managed by other control strategies. The biosynthesis pathway of validamycin A involves the *valC* gene, functioning as a C₇-cyclitol kinase.²

Over the past few decades, numerous strains of such antibiotic producing organisms have been isolated from diverse geographical regions.^{4,5} The classical culture and biochemical methods have been the conventional approaches used in the screening of antibiotic producing bacteria. The major limitations of these assays are that the test methods repeatedly use similar target organisms. Expensive and time consuming taxonomic studies are often required for identifying and characterizing the microorganism, after the biochemical confirmation. Rational selection of microorganisms by chemical or genetic fingerprinting provides a way to exclude

previously isolated organisms from screening programs and thus, overcomes the problems of repetition.

Recently, molecular techniques have been used to detect these functional genes present within bacterial communities.⁶ After screening of an antibiotic producing bacterium and the responsible gene, various molecular studies and genetic manipulations can be performed to improve the activity. The isolated gene can be re-engineered and cloned to increase the antibiotic production. Genetic information of such genes is also important to study the antibiotic resistance.

In this regard, we designed and fabricated a microfluidic platform which is capable of screening and amplifying a target gene based on a continuous flow polymerase chain reaction (PCR) phenomenon using specific primers. The amplified gene can later be detected and quantified using on-chip electrochemical methods thereby leading to a self-sustained lab-on-a-chip (LOC). This on-chip PCR consumes much less sample and time to amplify and detect the gene than a conventional thermal cycler. A typical gene amplification and detection take about 1–2 days, but it has been performed in 70 min on our micro-analytical system. The fabricated microchip was employed to isolate, amplify and detect the validamycin A producing gene. For specific detection of the amplified gene, several step-modified gold electrodes with streptavidin at the terminal and biotin-tagged primers were utilized to produce an enhanced signal.

2. Materials and methods

2.1 Reagents and materials

The target DNA was extracted from transgenic *Escherichia coli* cloned with the *valC* gene. Biotinylated primers for *valC* gene amplification with the following base sequences: 5'-biotin-GTA

^aSchool of Electronic and Electrical Engineering, Sungkyunkwan University, Seobu-Ro 2066, Suwon, Gyeonggi, 440-746, Republic of Korea. E-mail: yongsang@skku.edu; Fax: +82-31-290-5828; Tel: +82-31-299-4323

^bDepartment of Chemistry, Soongsil University, Sangdo-Ro 369, Seoul 156-743, Republic of Korea. E-mail: extant@ssu.ac.kr; Fax: +82-2-824-4383; Tel: +82-2-820-0431

CGT CCG CAT ACC CAC GAC CCT GAT C-3' (forward primer) and 5'-biotin-CAT CTC CAC GCT GGG TGA GAA GGA GTG-3' (reverse primer) were used. Primers for *valC* were designed to amplify an 800 bp genomic region in the template DNA. 1 kb plus step DNA ladder and 100 bp step DNA ladder were used as DNA rulers (Bionics, Korea). Cystamine dihydrochloride, glutaraldehyde, streptavidin (from *Streptomyces avidinii*), bovine serum albumin (BSA) and potassium ferrocyanide [$K_4Fe(CN)_6$] were of analytical grade. Deionized water (DI water) and phosphate buffer (PBS) (0.2 M, pH 6.6) were used throughout the experiment.

2.2 Device fabrication

The integrated microchip was composed of a serpentine microchannel and an electrochemical cell engraved in a polydimethylsiloxane (PDMS) layer. The detection electrodes were deposited on the indium tin oxide (ITO) coated glass substrate (Fine chemicals, Korea). ITO was used as a microheater for thermal heating due to its property of showing linear variation in its temperature by application of DC power.

To fabricate the ITO microheater, a positive photoresist (PR) (AZ-1512, Micro-Chem, USA) was spin-coated on the ITO side of the glass and then patterned using photolithography to cover the regions meant for different temperatures. The remaining ITO film was then etched using the $FeCl_3/HCl$ solution and the photoresist was removed using acetone. Au electrodes for cyclic voltammetry were designed and deposited over the non-ITO side of glass, using photolithography and the evaporation method. A positive PR layer was first spin coated on the opposite side of a cleaned ITO patterned glass wafer and exposed to UV light through a photomask containing the electrode design. Subsequently, a 50 nm Ti layer and a 320 nm thick Au layer were deposited on this glass wafer using a vacuum thermal evaporator. Then, the patterned positive photoresist was removed by ultrasonication in acetone.

The microchannels used in this study were molded in the PDMS (Dow corning, USA) polymer using the negative molding method. For this purpose, a 120 μm thick negative photoresist (SU-8 2075, Micro-Chem, USA) was spin-coated and patterned on a silicon wafer. A degassed mixture of a Sylgard 184 silicone elastomer and a curing agent (in 10 : 1 v/v ratio) was poured on the SU-8 patterned wafer and cured for 4 h at 75 °C. The thus formed PDMS mold was peeled off manually and drilled to make access holes of 3 mm diameter each. For finalizing the device fabrication steps, the PDMS mold and glass substrate containing ITO/Au electrodes were bonded with each other by UV-ozone treatment, keeping the Au electrode side of the glass in contact with PDMS.

2.3 Temperature control for the PCR microchip

The temperature zones for PCR of the *valC* gene were set to 94, 55 and 72 °C for denaturation, annealing and extension, respectively. To achieve the desired temperatures, a calibrated DC power was applied to the ITO heaters.⁷ The temperature was optimized by applying different sets of DC power to the ITO electrode while DI water was flowed at the rate of 3 $\mu L min^{-1}$ using a syringe pump. The temperatures of the zones were

measured using the thermocouple (CHAL-001, Omega, USA) specially bonded between the microchannels and the glass substrate.⁸ The power at separate electrodes had a synergistic effect on temperatures of different zones and was fixed to be 3640, 884 and 2940 mW for 94, 55 and 72 °C, respectively.

2.4 Microchannel treatment and electrode functionalization

Prior to PCR, the inner surface of the PDMS microchannel was treated by flowing 0.1 N HCl and 0.1 N NaOH for 5 minutes, respectively. After the acid/base treatment, DI water was pumped to clean the channel and then BSA was injected to coat the surface of the microchannel. Finally, the channel was cleaned again with DI water to remove the leftover BSA.

After the microchannel treatment, the Au electrode in a triangle shaped microchamber was cleaned by repetitive potential cycles between -0.2 and 1.2 V in 50 mM KOH (scan rate, $0.05 V s^{-1}$) until a stable cyclic voltammogram was obtained. After electrochemical cleaning, 50 mM cystamine dihydrochloride was injected through the modification inlet and incubated for 24 h in the dark at room temperature (RT) and subsequently rinsed with phosphate buffer. Following the cystamine dihydrochloride binding on the Au electrode, 10% glutaraldehyde was introduced and incubated in the same way for 12 h at RT. The surface of the glutaraldehyde–cystamine/Au electrode, now containing exposed aldehyde moieties, was reacted with streptavidin for 4 h at 4 °C to obtain a self-assembled streptavidin modified electrode (streptavidin–glutaraldehyde–cystamine/Au).⁹

2.5 Electrochemical measurements

In this study, cyclic voltammetry (CV) measurement and electrochemical impedance spectroscopy (EIS) were carried out with CHI 800B and CHI 660B electrochemical analyzers (CH Instruments Inc., USA), respectively. The sequentially modified working Au electrodes and Au counter and reference electrodes were used for the measurement. Each step of electrode modification was confirmed and characterized using CV and EIS. CV after each modification step was performed in 5 mM $K_4Fe(CN)_6$ prepared in PBS buffer at a scan rate of $20 mV s^{-1}$ within a potential range of -0.4 to 0.6 V. The EIS measurement was performed under similar conditions within a frequency range of 10^4 to 1 Hz.

The final electrochemical detection of the streptavidin/biotin–DNA conjugate was performed in PBS buffer using CV. This CV was carried out within a scan range of 0 to 1.2 V at a scan rate of $10 mV s^{-1}$.

2.6 Microchip operation

The overall experimental procedure was carried out using the following pathway. After the microchannel surface treatment and Au electrode modification, a calibrated DC bias was applied to the ITO electrodes laid on the backside of the glass substrate for heating the denaturation, annealing and extension PCR zones. To start the PCR, a mixture of template DNA, biotinylated primers and a pre-PCR mixture containing dNTPs, DNA polymerase, reaction buffer, and $MgCl_2$ (total volume: 50 μL) was injected into the inlet through a silicone tube using a syringe

pump at the flow rate of $3 \mu\text{L min}^{-1}$. In this zone, the amplification of the target gene took place with the help of the enzyme and cyclic change in temperature. Finally after amplification, the amplicon was pumped into the electrochemical cell and the extra sample was allowed to pass to the outlet reservoir, which can be used for further analysis. Inside the electrochemical cell, the biotin conjugated DNA amplicon was left to bind with streptavidin for 30 min. After the designated time, the leftover DNA sample was sucked out using a syringe and the cell was filled with PBS buffer. Finally the CV was carried out to detect the amplified DNA.

3. Results and discussion

3.1 Microchip design

The image of the integrated microchip is shown in Fig. 1. The microchip was fabricated using standard photolithographic

procedures on a $96 \text{ mm} \times 96 \text{ mm} \times 0.7 \text{ mm}$ glass substrate. The microchip was disposable and meant for single use only. Microchannels were cast in the PDMS layer by a negative molding technique. The width and depth of the microchannel created were $250 \mu\text{m}$ and $120 \mu\text{m}$, respectively, with 2950 mm length for 30 cycles. A continuous flow system transports the PCR mixture through different pre-fixed temperature zones for PCR. Compared to a stationary chamber based format, the continuous system approach provides faster thermal cycling because thermal inertia depends on the thermal mass of the sample, rather than the chip. In this system, the required heating and cooling sequence and the residence time were controlled by channel routing and flow speed.¹⁰ Each zone for denaturation, extension and annealing measured an area of 1150 , 1250 and 1150 mm^2 , respectively. The length of the channel for extension in each cycle was double those of the other zones. A larger extension zone assured longer residence time of the sample within this zone. The PCR module also contained provision for pre-PCR denaturation and final extension. The gaps between the temperature zones ensured efficient cooling of the circulating liquid in between them. Recently Peham *et al.* reported the use of Peltier devices attached with metal blocks to fabricate PCR. Such types of devices are rather far from miniaturization, and make the process tedious.¹¹ In contrast, the patterned ITO heater used in this work enables the realization of a handheld device on a monolithic chip. PDMS is also cost effective compared to other reports, in which a SU-8 based microchannel¹² or a silicon based device¹³ was used. The electrochemical cell had a total volume of $\sim 10 \mu\text{L}$. The dimensions of the Au working electrode were $3 \text{ mm} \times 3 \text{ mm}$ while counter and reference electrodes had a length and a width of $4 \text{ mm} \times 1 \text{ mm}$.

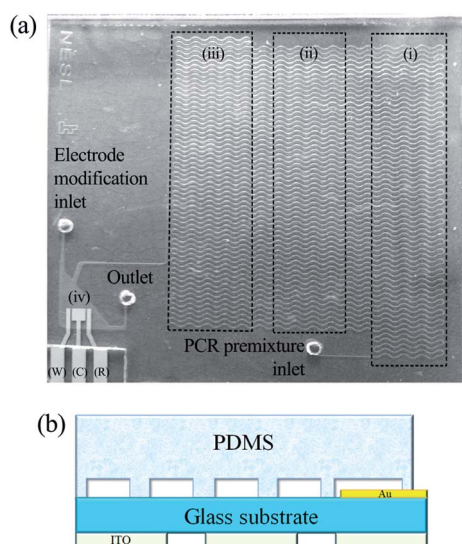


Fig. 1 Integrated microchip. (a) Photograph of the integrated chip. The dotted line marks the ITO based heating zone (i) denaturation, (ii) annealing and (iii) extension; (iv) electrochemical cell showing working (W), counter (C) and reference (R) electrodes. (b) Cross sectional schematic of the device.

3.2 Microchannel treatment and electrode functionalization

The PDMS surface has an affinity to bind with biomolecules.^{14,15} Thus, PCR within an untreated microchannel will lead to an insufficient amplification due to binding of polymerase and other biomolecules to the inner surface of the PDMS microchannel. Acid/base and BSA treatment of the microchannel

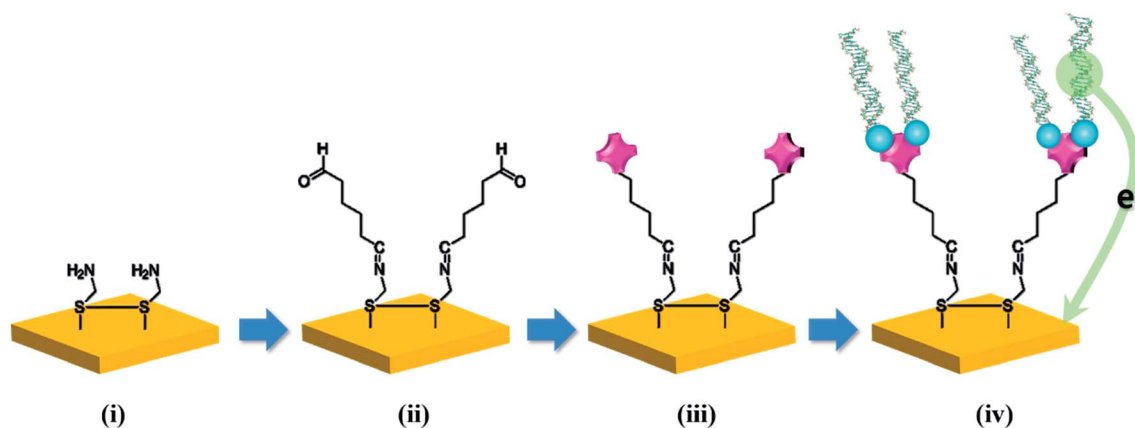


Fig. 2 Schematic image of the Au electrode modification process. (i) 50 mM cystamine dihydrochloride deposition for 24 h in the dark at RT; (ii) 10% glutaraldehyde deposition for 12 h at RT; (iii) streptavidin deposition for 4 h at $4 \text{ }^\circ\text{C}$; (iv) biotinylated DNA amplicon bound on the modified Au electrode by streptavidin–biotin interaction.

helped in preventing this erroneous amplification.^{16,17} Ionic treatment of the channel neutralized the inner charge of the PDMS microchannel while the injected BSA coated the microchannel surface. With these modifications, no free PDMS surface was left to bind with polymerase and other biomolecules.

The functionalization scheme of the Au electrode is summarized in Fig. 2. In short, the thiol group of cystamine dihydrochloride reacted with the Au surface to form a self-aligned monolayer.¹⁸ Later, one end of the glutaraldehyde bonded with the amine group of cystamine dihydrochloride while the other end bonded with streptavidin. The rinsing of excess cystamine dihydrochloride prevented its reaction with glutaraldehyde, resulting in solid mass formation. Glutaraldehyde easily binds with any protein through its amine group. To avoid the contamination of the PCR microchannel, glutaraldehyde was carefully introduced into the electrochemical cell. Finally with these modifications, the Au electrode had a streptavidin terminal end to bind specifically with the biotin conjugated DNA amplicon.¹⁹ Recently Moscovici *et al.* also reported a similar technique for the detection of prostate cancer cells.²⁰ Alternatively, Feng Li and coworkers proposed a gold surface modification protocol based on the self-assembly of gold nanoparticles on a mercapto-diazoaminobenzene monolayer modified electrode for the electrochemical sensing of DNA. Although this modification increased the sensing efficiency, the protocol is excessively complicated and time consuming.²¹

Confirmation of each modification was performed using CV and EIS. Fig. 3(a) shows the cyclic voltammograms of the Au electrode in 5 mM $K_4Fe(CN)_6$. CV of $K_4Fe(CN)_6$ using the Au electrode after each modification gave different electrochemical responses. The current signal from $K_4Fe(CN)_6$ reduced consequently due to the binding of molecules on the Au electrode and less availability of free Au which confirms the functionalization of working electrodes. To further investigate the feasibility of the electrochemical assay, the EIS of electrodes was carried out under the same conditions. As shown in Fig. 3(b), the similar results were obtained using EIS. The bare Au surface exhibited a relatively straight line, attributing to a free electron transfer process. After the surface was treated with cystamine dihydrochloride, a significant increase of the electron transfer resistance was seen leading to a larger semicircle.

3.3 On-chip PCR

At the desired zonal temperature level, the mixture of template DNA, biotinylated primers and the pre-PCR mixture containing dNTPs, DNA polymerase, reaction buffer, and $MgCl_2$ was subjected to PCR amplification on the microchip. The reaction mixture was injected at an optimized flow rate of $3 \mu L \text{ min}^{-1}$ using a syringe pump, which took about 40 min for 30 cycles. The primer set used, amplified an 800 bp target of the *valC* gene responsible for the synthesis of the antifungal antibiotic validamycin A.

Different initial concentrations of the template DNA were used to check the efficacy of our PCR microchip. The DNA amplicon obtained in this way was verified by conventional slab agarose gel electrophoresis for the presence of the desired

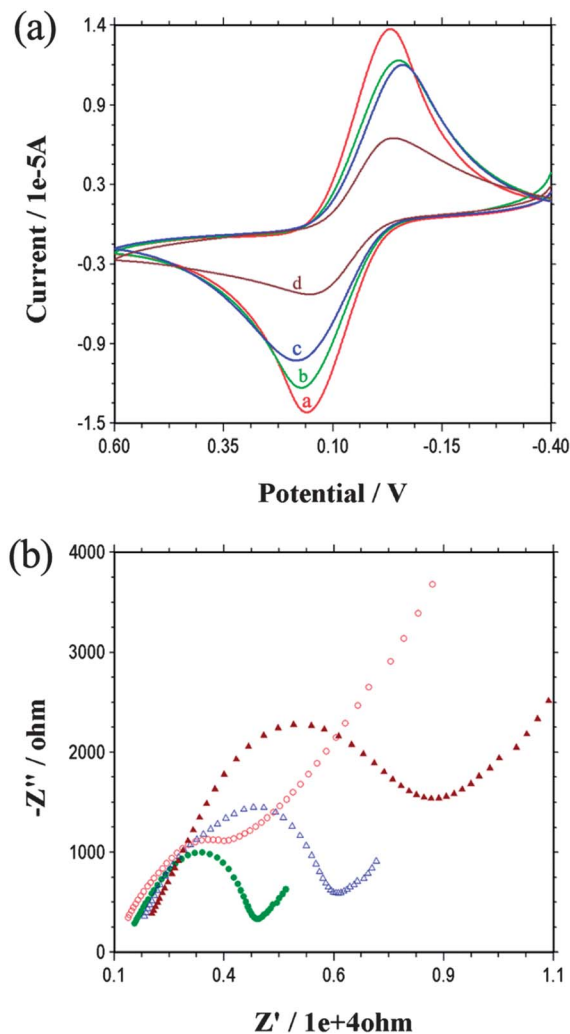


Fig. 3 Electrochemical verification of the Au electrode modification process. (a) CV of the Au electrode in 5 mM $K_4Fe(CN)_6$ at a scan rate of 20 mV s^{-1} within a potential range of -0.4 to 0.6 V ; curve a: bare gold, curve b: cystamine dihydrochloride, curve c: glutaraldehyde, and curve d: streptavidin; (b) EIS measurement, performed under similar conditions to (a) within a frequency range of 10^4 to 1 Hz . Red (open circle): bare Au electrode; green (solid circle): cystamine; blue (open triangle): glutaraldehyde; brown (solid triangle): streptavidin.

product. A conventional PCR amplification of the target DNA was also performed for verification. Fig. 4 shows the gel-doc image of agarose gel electrophoresis for different amplified products. Lane 1 of Fig. 4(a) represents the target amplicon obtained using the microchip from a $30 \text{ ng } \mu L^{-1}$ initial template DNA concentration whereas lane 2 shows the amplicon from conventional PCR amplification. As clearly seen, the microchip produced a higher amount of amplified DNA as a result of continuous dynamic mixing of the reaction mixture, which is not available in a typical thermal cycler. Lanes 3, 4 and 5 represent the amplicon obtained using the microchip from $3 \text{ ng } \mu L^{-1}$, 300 and $30 \text{ pg } \mu L^{-1}$ of initial template DNA concentration. For the negative control, amplification of lambda phage DNA and *E. coli* was performed using the primers meant for the *valC* gene. As anticipated, no product was obtained from lambda phage DNA, which is confirmed in lane 6 of Fig. 4(a) and lane 1

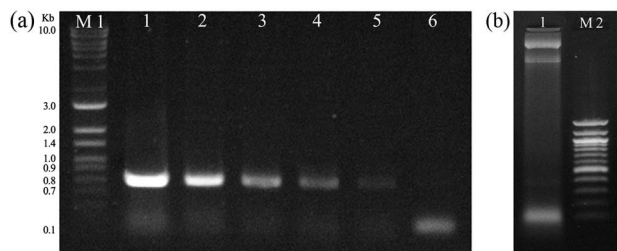


Fig. 4 (a) Gel-DOC image of amplicons from different initial template concentrations and control cases. M1: 1 kb plus step DNA ladder; lane 1: amplicon of 30 ng μL^{-1} template using on-chip PCR; lane 2: amplicon of 30 ng μL^{-1} template using conventional PCR; lane 3: amplicon of 3.0 ng μL^{-1} template using on-chip PCR; lane 4: amplicon of 300 pg μL^{-1} template using on-chip PCR; lane 5: amplicon of 30 pg μL^{-1} template using on-chip PCR; lane 6: amplicon of Lambda phage DNA for negative control; (b) gel-doc image, lane 1: amplicon of *E. coli* DNA for negative control; M2: 100 bp step DNA ladder.

of Fig. 4(b). This result proved the efficacy of the device showing no non-specific amplification. The amplified product was later analyzed using a voltammetric electrode for verification and quantification.

3.4 Electrochemical detection of DNA

As mentioned in Section 3.2, the modification of the Au electrode surface was carried out to capture specifically the amplified target gene. Electrochemical measurement of each amplicon resulting from the different initial template concentrations was carried out within a scan range of 0 to 1.2 V at a rate of 10 mV s^{-1} in PBS buffer. The complete experimental flow of DNA amplification and detection of each concentration was performed on fresh devices and at least thrice to check the reproducibility of the proposed method. The guanosine present in the amplicon DNA released electrons upon electrochemical oxidation, and they passed to the gold working electrode through the linkers. The oxidation of guanosine is a two-step mechanism involving the loss of two electrons in each step. The higher the amount of amplified DNA present at the electrode, the more the guanosine underwent electrochemical oxidation. Fig. 5 shows the cyclic voltammogram of products obtained from different initial template DNA concentrations. The amplicon from 30 ng μL^{-1} initial template DNA concentration produced an oxidation peak at 0.93 V for guanosine, with a current level of -6.87×10^{-7} A. The oxidation peak obtained was in accordance with the previously reported value.²² Similarly other amplified products also produced an oxidation peak at 0.93 V with a corresponding decrease in the current level. A calibration curve was plotted for the results obtained, which is shown in Fig. 5(b). A relative linear current response was obtained which could be useful for detecting unknown DNA concentrations ($n = 3$, correlation coefficient, $R^2 = 0.989$).

Each modification step helped in better and specific amplification of the signal. Monolayers of cystamine dihydrochloride increased the total surface area of the electrode, which resulted in higher binding sites for the DNA. Glutaraldehyde is a well-known electroactive linker which bridges the two amine groups efficiently. The streptavidin–biotin complex represents the highest affinity noncovalent interaction in nature. This fact

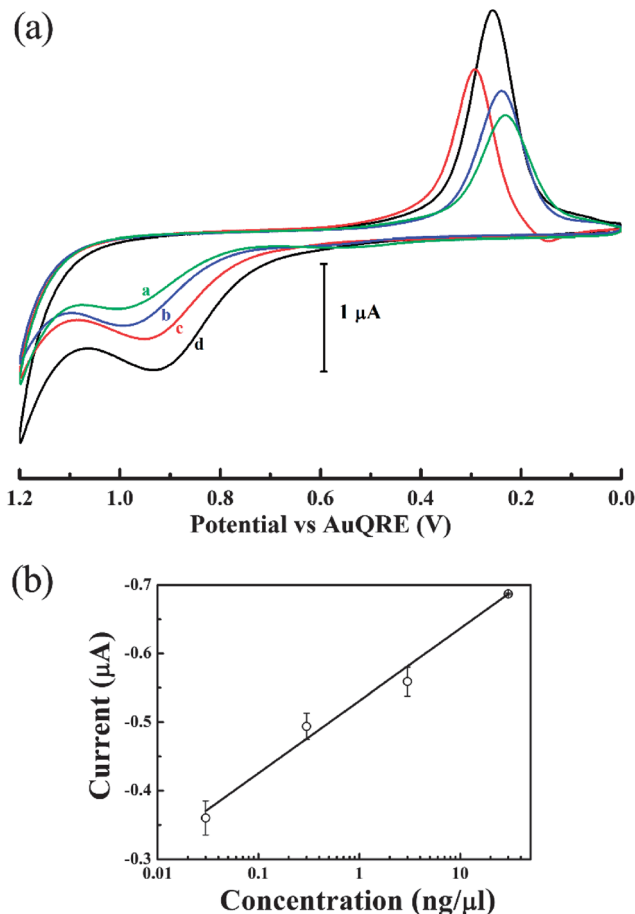


Fig. 5 Cyclic voltammograms of amplicons from different initial template DNA concentrations. (a) CV was carried out within a scan range of 0 to 1.2 V at a scan rate of 10 mV s^{-1} in PBS buffer, curve a: 30 pg μL^{-1} of initial template DNA, curve b: 300 pg μL^{-1} of initial template DNA, curve c: 3.0 ng μL^{-1} of initial template DNA, and curve d: 30 ng μL^{-1} of initial template DNA. (b) Relationship between amplicons from different initial template DNA concentrations and the average electrochemical signal ($n = 3$); error bar represents standard deviation ($R^2 = 0.989$).

makes streptavidin–biotin a universal coupling system in biosensors.^{23,24} This obvious fact was also confirmed during our experiment. Continuous voltammetry for multiple cycles produced no change in oxidation peak or current response, which makes our system a very stable platform.

Typically in most of the integrated PCR chips, post-PCR processes carry out optical detection based on the fluorescence scanning of the biomolecule tagged with the reporter dye.^{25,26} In many cases, the fluorescent dye used for detection inhibits the PCR either by preferentially binding at certain regions of template DNA or altering their melting curve or inhibiting the activity of the enzyme, resulting in decreased amplification efficiency.²⁷ Moreover the optical detection system consists of several submodules such as the laser source, lenses and the photomultiplier tube, which make the system hefty and highly expensive.

Alternatively, the electrochemical detection method relies on a relatively simple technique with use of only 3 electrodes, and can be fabricated (or miniaturized) on a chip. Few other groups

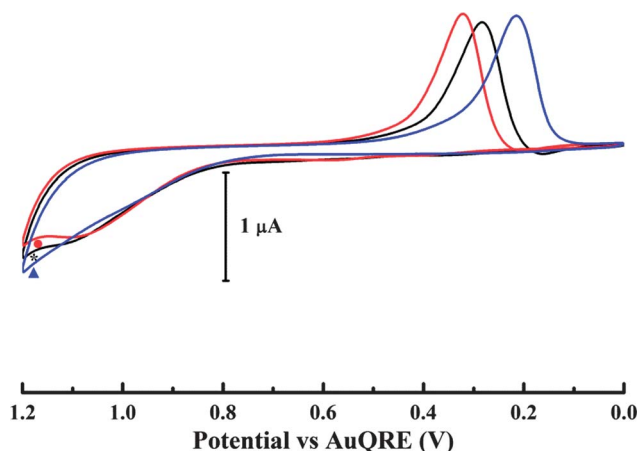


Fig. 6 Cyclic voltammograms of negative controls. CV was carried out within a scan range of 0 to 1.2 V at a scan rate of 10 mV s^{-1} in PBS buffer (0.2 M, pH 6.6). (●) Amplicon of the Lambda phage template using non-biotinylated primers; (*) biotinylated primers; (▲) PBS buffer.

have also reported the integration of electrochemical detection for PCR amplicons, which proved to be advantageous. For the determination, Yeung *et al.* microfabricated ITO electrodes while Ferguson *et al.* used gold as working electrode,^{28,29} and similarly Yamanaka and co-workers used a disposable printed electrode chip for amplicon detection.³⁰

The voltammetric peak obtained was only due to the binding of the amplified DNA product and not because of the binding of unused biotinylated primers. To demonstrate this, we performed a control voltammetry of the pre-PCR mixture along with primers, sans the template DNA. The mixture resulted in a noticeable voltammetric peak. The curve (▲) in Fig. 6 represents blank voltammetry of only PBS buffer while the curve (*) shows the control voltammetry of PCR primers. As a negative control, PCR amplicons of lambda phage DNA using non-biotinylated primers from a bench top thermal cycler showed no current response, which was well expected (Fig. 6 curve (●)).

4. Conclusion

We developed a microchip integrating two useful systems *i.e.* molecular analysis based on PCR and electrochemical detection for the screening of genes. The device was validated by amplifying and detecting the *valC* gene responsible for validamycin A biosynthesis. Effective integration of DNA amplification and electrochemical detection was successfully demonstrated here. Specific modification of the electrode proved essential for the detection. The fabricated chip exhibited high sensitivity and good selectivity for *valC* gene analysis. The ability to screen and detect the antibiotic producing gene can be useful to obtain a novel antibiotic, to tackle the ever-growing problem of multi-drug resistance in pathogens.

Acknowledgements

This research was supported by Basic Science Research Program through the National Research Foundation of Korea funded by the Ministry of Science, ICT & Future Planning (NRF-2011-

0024786); and Business for Cooperative R & D between Industry, Academy, and Research Institute funded by Korea Small and Medium Business Administration in 2013 (C0119656).

References

- G. D. Robson, P. J. Kuhn and A. P. Trinci, *J. Gen. Microbiol.*, 1988, **134**, 3187–3194.
- K. Minagawa, Y. Zhang, T. Ito, L. Bai, Z. Deng and T. Mahmud, *ChemBioChem*, 2007, **8**, 632–641.
- T. Mahmud, *Nat. Prod. Rep.*, 2003, **20**, 137–166.
- K. Tiwari and R. K. Gupta, *Crit. Rev. Biotechnol.*, 2012, **32**, 108–132.
- M. L. Lemos, A. E. Toranzo and J. L. Barja, *Microb. Ecol.*, 1985, **11**, 149–163.
- L. Yuan, J. H. Liu, G. Z. Hu, Y. S. Pan, Z. M. Liu, J. Mo and Y. J. Wei, *J. Med. Microbiol.*, 2009, **58**, 1449–1453.
- S.-R. Joung, C. J. Kang and Y.-S. Kim, *Jpn. J. Appl. Phys.*, 2008, **47**, 1342–1345.
- S. K. Jha, R. Chand, D. Han, Y.-C. Jang, G.-S. Ra, J. S. Kim, B.-H. Nahm and Y.-S. Kim, *Lab Chip*, 2012, **12**, 4455–4464.
- K.-A. Yoo, K.-H. Na, S.-R. Joung, B.-H. Nahm, C. J. Kang and Y.-S. Kim, *Jpn. J. Appl. Phys.*, 2006, **45**, 515–518.
- M. U. Kopp, A. J. Mello and A. Manz, *Science*, 1998, **280**, 1046–1048.
- J. R. Peham, W. Griener, H. Steiner, R. Heer, M. J. Vellekoop, C. Nohammer and H. Wiesinger-Mayr, *Biomed. Microdevices*, 2011, **13**, 463–473.
- T. B. Christensen, D. D. Bang and A. Wolff, *Microelectron. Eng.*, 2008, **85**, 1278–1281.
- T. M.-H. Lee, M. C. Carles and I. M. Hsing, *Lab Chip*, 2003, **3**, 100.
- H. Makamba, J. H. Kim, K. Lim, N. Park and J. H. Hahn, *Electrophoresis*, 2003, **24**, 3607–3619.
- M. W. Toepke and D. J. Beebe, *Lab Chip*, 2006, **6**, 1484.
- K. S. Shin, Y. H. Kim, J. A. Min, S. M. Kwak, S. K. Kim, E. G. Yang, J. H. Park, B. K. Ju, T. S. Kim and J. Y. Kang, *Anal. Chim. Acta*, 2006, **573–574**, 164–171.
- J. C. McDonald, D. C. Duffy, J. R. Anderson, D. T. Chiu, H. Wu, O. J. Schueller and G. M. Whitesides, *Electrophoresis*, 2000, **21**, 27–40.
- M. Wirde, U. Gelius and L. Nyholm, *Langmuir*, 1999, **15**, 6370–6378.
- K.-H. Na, Y.-S. Kim and C. J. Kang, *Ultramicroscopy*, 2005, **105**, 223–227.
- M. Moscovici, A. Bhimji and S. O. Kelley, *Lab Chip*, 2013, **13**, 940.
- F. Li, Y. Feng, P. Dong and B. Tang, *Biosens. Bioelectron.*, 2010, **25**, 2084–2088.
- Y.-C. Jang, S. K. Jha, R. Chand, K. Islam and Y.-S. Kim, *Electrophoresis*, 2011, **32**, 913–919.
- Y. K. Jung, T. W. Kim, C. Jung, D.-Y. Cho and H. G. Park, *Small*, 2008, **4**, 1778–1784.
- N. Nath and A. Chilkoti, *Anal. Chem.*, 2002, **74**, 504–509.
- P. J. Obeid and T. K. Christopoulos, *Anal. Chim. Acta*, 2003, **494**, 1–9.

- 26 G. V. Kaigala, V. N. Hoang, A. Stickel, J. Lauzon, D. Manage, L. M. Pilarski and C. J. Backhouse, *Analyst*, 2008, **133**, 331.
- 27 H. Gudnason, M. Dufva, D. D. Bang and A. Wolff, *Nucleic Acids Res.*, 2007, **35**, e127.
- 28 S. S. Yeung, T. M. Lee and I. M. Hsing, *Anal. Chem.*, 2008, **80**, 363–368.
- 29 B. S. Ferguson, S. F. Buchsbaum, J. S. Swensen, K. Hsieh, X. Lou and H. T. Soh, *Anal. Chem.*, 2009, **81**, 6503–6508.
- 30 K. Yamanaka, M. Saito, K. Kondoh, M. M. Hossain, R. Koketsu, T. Sasaki, N. Nagatani, K. Ikuta and E. Tamiya, *Analyst*, 2011, **136**, 2064.